

Supplementary Materials for  
**Immunopeptidome analysis reveals SERPINB3 as an autoantigen driving  
eczematized psoriasis**

Manja Jargosch *et al.*

Corresponding author: Natalie Garzorz-Stark, [natalie.garzorz-stark@uniklinik-freiburg.de](mailto:natalie.garzorz-stark@uniklinik-freiburg.de)

*Sci. Adv.* **11**, eadx0637 (2025)  
DOI: 10.1126/sciadv.adx0637

**The PDF file includes:**

Supplementary Materials and Methods  
Figs. S1 to S13  
Tables S1 to S4  
Legends for files S1 and S2  
References

**Other Supplementary Material for this manuscript includes the following:**

Files S1 and S2

## **SUPPLEMENTARY MATERIALS AND METHODS**

### **Mass spectrometry of immunoaffinity purified HLA ligands**

*Validation of experimental SERPINB3 and SERPINB4 spectra by heavy isotope-labeled synthetic peptides:*

A total of 16 SERPINB3 as well as SERPINB4 peptides exclusively eluted from HLA class I or II molecules of psoriatic skin biopsies were subjected to spectral validation. Heavy isotope-labeled synthetic peptides (valine- $^{13}\text{C}_5, ^{15}\text{N}$ ; alanine- $^{13}\text{C}_3, ^{15}\text{N}$ ; threonine- $^{13}\text{C}_4, ^{15}\text{N}$ ; isoleucine- $^{13}\text{C}_6, ^{15}\text{N}$ ; or leucine- $^{13}\text{C}_6, ^{15}\text{N}$ ; FQQFRKSKENNIF without heavy isotope label) were synthesized in-house by solid-phase peptide synthesis (Wirkstoffpeptidlabor, Department of Immunology, University of Tübingen). Peptides were spiked at  $\sim 100$  fmol/ $\mu\text{l}$  into a complex matrix of HLA class I or II peptides eluted from the B-lymphoblastoid cell line JY. Mass spectrometric data was acquired and analyzed as described above, while permitting the respective heavy isotope label as additional dynamic modification. Sequence identity of experimental and synthetic peptides was verified by manual comparison of fragment spectra.

### **HLA typing**

HLA class I and II typing for HLA-A, -B, -C, -DRB1, -DRB3, -DRB4, -DRB5, -DQA1, -DQB1, -DPA1, and -DPB1 on 4-digit level was performed at HistoGenetics LLC (Ossining, USA) by sequencing DNA isolated from peripheral blood mononuclear cells (PBMCs) of selected patients.

### **Bulk RNA sequencing and Gene Set Enrichment Analysis (GSEA) of skin biopsies**

Bulk RNA sequencing was performed as described previously (77). In brief, RNA from skin biopsies was isolated using QIAzol Lysis Reagent (Qiagen) and miRNeasy Mini Kit (Qiagen). Libraries were generated using the TruSeq Stranded Total RNA Kit (Illumina) according to manufacturer's high sample protocol. Samples were sequenced on an Illumina HiSeq4000 as paired-end with a read length of 2x 150 bp and an average output of 40 Mio reads per sample and end. Sequence alignment was performed using STAR aligner with human genome reference hg38. RNAseq count data were normalized and then transformed using variance stabilizing transformation (VST) from the Bioconductor package DESeq2 (normalized gene counts) (78). Differentially expressed genes (DEGs) between lesional and non-lesional

skin within each disease group were also calculated with DESeq2. Gene set enrichment analysis (GSEA) for EczPso was performed on log2FC ranked genes using the pathways of Reactome. GSEA plots were generated with R package "enrichplot" and function "cnetplot". Patient characteristics of the RNAseq cohort are listed in Table S2.

### **Production of murine recombinant Serpinb3b**

*Cloning and generation of recombinant baculovirus:* *Serpinb3b* gene strand was synthesized by Eurofins Genomics carrying at the N-terminus a leading sequence for extracellular matrix, a 10-fold His-tag for purification and a V5-tag for unambiguous identification. The construct was digested and ligated with pAcGP67B-vector (BD). Recombinant baculovirus was generated by co-transfecting adherent Sf9 cells (Thermo Fisher Scientific) with ProGreen™-Baculovirus DNA (AB Vector, A1) and *Serpinb3b*-pAcGP67B plasmid according to the manufacturer's instructions.

*Production of recombinant Serpinb3b:* Recombinant *Serpinb3b* was produced using the baculovirus-mediated insect cell expression system. In short, Sf9 wild type cells were maintained at 27°C in Insect-XPRESS protein-free insect cell medium (Lonza, BELN12-730Q) with L-glutamine and 10 µg/mL gentamycin sulphate solution (Carl Roth, 2475.1). Suspension cultures were inoculated with high titer recombinant baculovirus and incubated for 72 h. Using a nickel chelate affinity matrix (HisTrap excel, GE Healthcare Life Sciences, GE17-3712-05), the recombinant proteins were purified on an ÄKTA™ pure (GE Healthcare Life Sciences) system. After purification, diafiltration (PBS, pH = 7.4) was performed using 10 kDa cut-off Amicon® Ultra Centrifugal Filters (Merck Millipore, UFC801024). *Serpinb3b* was sterilized using Millex®-GP Syringe Filter Units (Merck Millipore, SLGP033RS) with 0.22 µm pore size. Purity was confirmed by SDS-PAGE in a 10 % Tris-Tricine gel and subsequent Coomassie Brilliant Blue staining (Fig. S13). Densitometric analysis of the stained gel revealed a high-purity exceeding 95 %. Endotoxin level was determined by ENDOLISA and resulted 0.0226 ng per 1 µg of protein.

### **Histology and immunohistochemistry**

Fixated skin tissue was embedded in paraffin. 5 µm sections were cut and dewaxed. After rehydration, sections were stained with haematoxylin and eosin using standard methods. For Immunohistochemistry

2.5 µm sections were used and staining's were performed by an automated BOND system (Leica) according to the manufacturer's instructions using following monoclonal antibodies: IL-17A (R&D systems, AF-317-NA, 1:40 in citrate buffer), KI-67 (Zytomed, RBG027, undiluted in EDTA buffer), NETs (Abcam, ab68672, 1:200 in citrate buffer), FcεRI (Abcam, ab54411, 1:75 in citrate buffer).

### **Isolation of lesional T cells from PsV and Ecz skin biopsies and production of supernatant**

Primary human lesional T cells were isolated from freshly taken skin biopsies of PsV (n=4) and Ecz (n=3) patients by emigration towards an IL-2 gradient followed by expansion with α-CD3/α-CD28 stimulation as described previously (79). Supernatants of expanded lesional T cells were generated by 3-day stimulation with 0.75 µg/mL α-CD3 (pre-coated, BD Biosciences) and 0.75 µg/mL soluble α-CD28 (BD Biosciences). A mixture of 4 PsV or 3 Ecz lesional supernatants at equimolar ratio was used 1:10 diluted for stimulation of keratinocytes. PsV and Ecz TCS were mixed 1:1 to generate PsV/Ecz TCS to mimic EczPso.

### **Immunofluorescence staining**

Sections of paraffin-embedded skin biopsy samples (5 µm, each) were air-dried overnight at 37 °C, deparaffinized, rehydrated and treated in a pressure cooker with 0.01 M sodium citrate buffer (pH 6.0) for 7 min. Slides were blocked with 10 % donkey serum (Abcam, ab7475) and/or goat serum (Abcam, ab7481) for 1 h at RT, and then incubated overnight at 4 °C with primary antibody, including monoclonal rat anti-human CD3 (Abcam, ab11089, diluted 1:50) and monoclonal mouse anti-human SERPINB3 (R&D Systems, MAB6528, 1:50). After washing with 0.05 M Tris-HCl buffer (pH 7.6), sections were incubated with secondary antibody (1:1000), including goat anti-rabbit Alexa-488-conjugated antibody (Invitrogen, A-32731), donkey anti-mouse Alexa-555-conjugated antibody (Invitrogen, A-31570), and goat anti-rat Alexa-647-conjugated antibody (Invitrogen, A-21247) for 1 h at RT. To reduce tissue auto-fluorescence, samples were treated with TrueVIEW auto fluorescence quenching KIT (Vector Laboratories, SP-8500) according to manufacturer's instructions. Nuclei were counterstained with DAPI (Sigma, 1:500). Slides were mounted in Vectashield anti-fade reagent (Vector Laboratories, H-1900) and examined using microscope slide scanner (Axio Scan.Z1 Zeiss, Germany) at 20x magnification.

Images were visualized and quantified as described before (80) using QuPath software, and individually evaluated by two trained dermatopathologists.

### **Pso/Ecz-Classifier**

The molecular classifier to distinguish between Pso and Ecz was conducted by gene expression analysis of *NOS2* and *CCL27* in RNA samples of lesional skin as mentioned before (81).

### **Bio-Plex analysis**

Cell-free supernatants derived from human T cell proliferation assays were analyzed for 27 cytokines, chemokines and growth factors using the Bio-Plex Pro Human Cytokine 27-plex Assay (Bio-Rad Laboratories, Hercules, Calif) according to the manufacturer's recommendation.

### **Western Blot analysis**

After stimulation, keratinocytes were lysed in RIPA lysis buffer (Santa Cruz) supplemented with 1 mM sodium orthovanadate, 2 mM PMSF and proteinase inhibitor cocktail (1:70) according to the manufacturer's instructions. Equal protein concentrations – determined by BCA protein assay – were resolved by SDS-PAGE using Bolt 4-12 % Bis-TrisPlus Gels and analyzed by Western Blot using enhanced chemiluminescence. For staining following antibodies were used:  $\alpha$ hSERPINB3 (R&D systems, MAB6528, 1:1,000),  $\alpha$ h $\beta$ -ACTIN (SIGMA, A2228, 1:10,000),  $\alpha$ HRP (Jackson, 115-035-166, 1:10,000) and  $\alpha$ hHSP60 (BD, 611562, 1:1,000).

### **Isolation of RNA, cDNA synthesis and qPCR**

RNA was isolated using QIAzol Lysis Reagent (Qiagen) and miRNeasy Mini Kit (Qiagen) for RNAlater preserved tissue or RNeasy Mini Plus Kit (Qiagen) for cell culture cells according to manufacturer's protocol. mRNA was transcribed into cDNA with Applied Biosystems High Capacity cDNA Reverse Transcription Kit (Thermo Fisher Scientific). Gene expression was measured on an Applied Biosystems

ViiA7 Real-Time PCR system (Thermo Fisher Scientific) using Fast Start Universal SYBRGreen Master Rox (Roche). Primers were ordered from Metabion (<http://www.metabion.com>) and are listed in supplementary Table S4. Data are shown as relative gene expression to control sample using  $2^{-(\Delta\Delta cT)}$  method and *18S* (for human samples) or *Gapdh* (for murin sampes) as housekeeper.

## SUPPLEMENTARY FIGURES

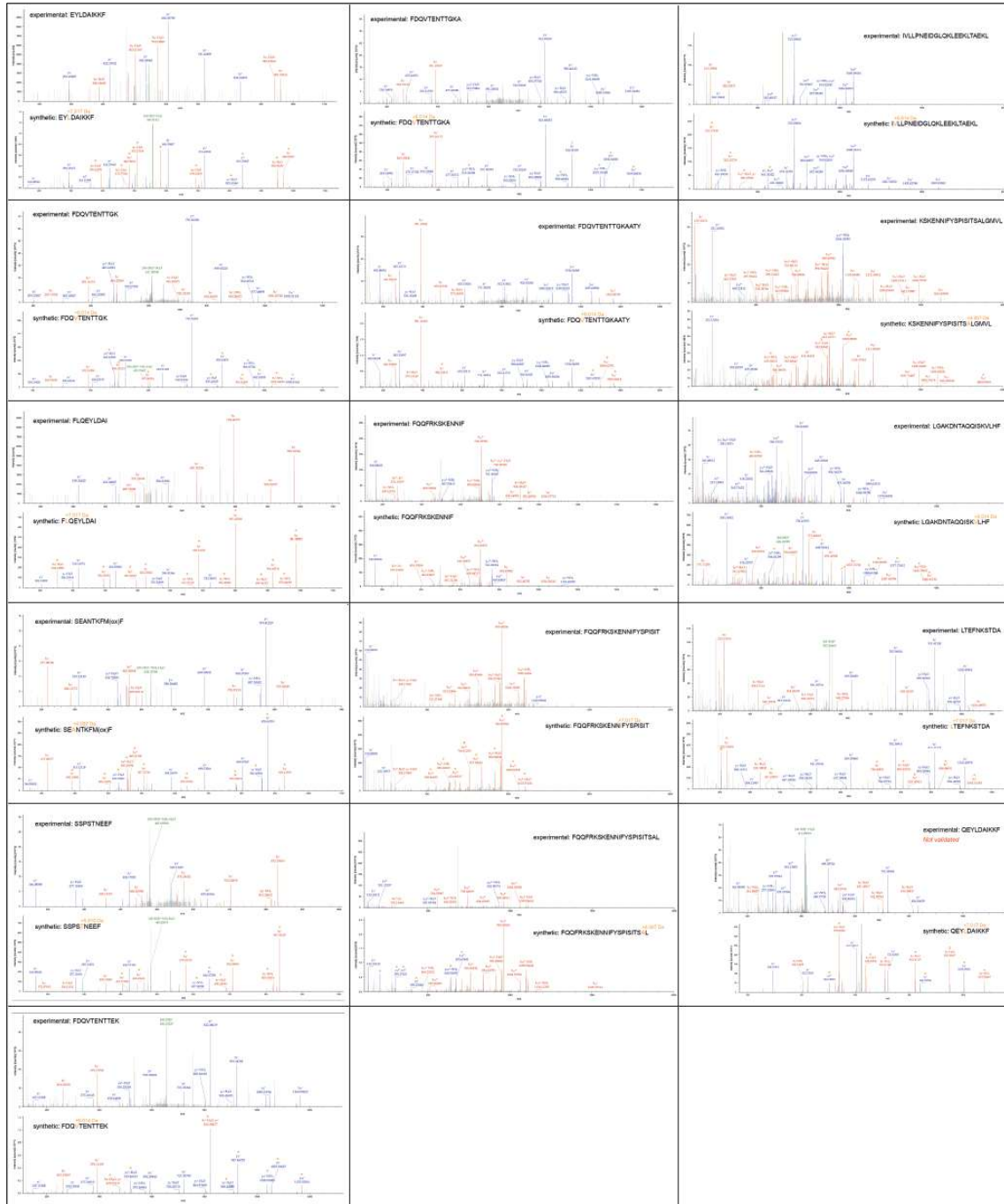


**Fig. S1: Validation of experimental SERPINB3/SERPINB4 fragment spectra by synthetic heavy isotope-labeled peptides.** The position of the heavy isotope label along with the corresponding mass shift are indicated in orange for each synthetic peptide sequence; dominant fragment ions including the labeled amino acid are marked with an asterisk. QEYLDAIKKF was the only peptide sequence not passing spectral validation.

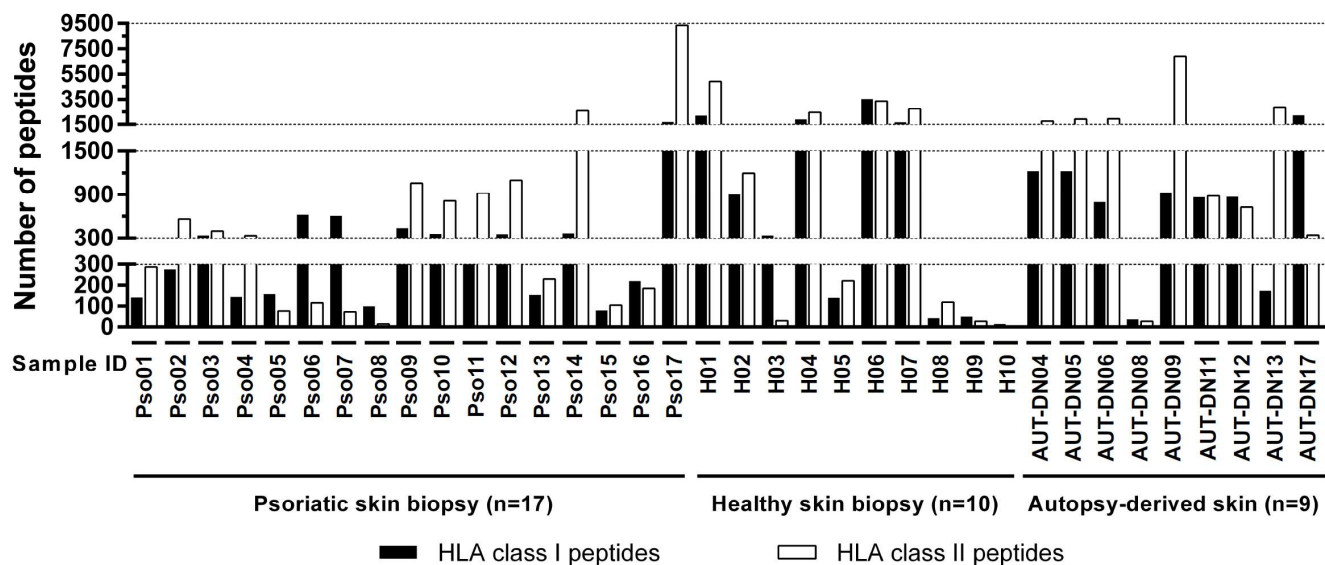


**Fig. S2: Number of peptides eluted from HLA class I and II molecules of psoriatic or healthy (H) skin biopsies as well as autopsy-derived (AUT-DN) skin.** Pso = psoriasis, H = healthy, AUT-DN = healthy autopsy-derived, HLA = human leukocyte antigen.



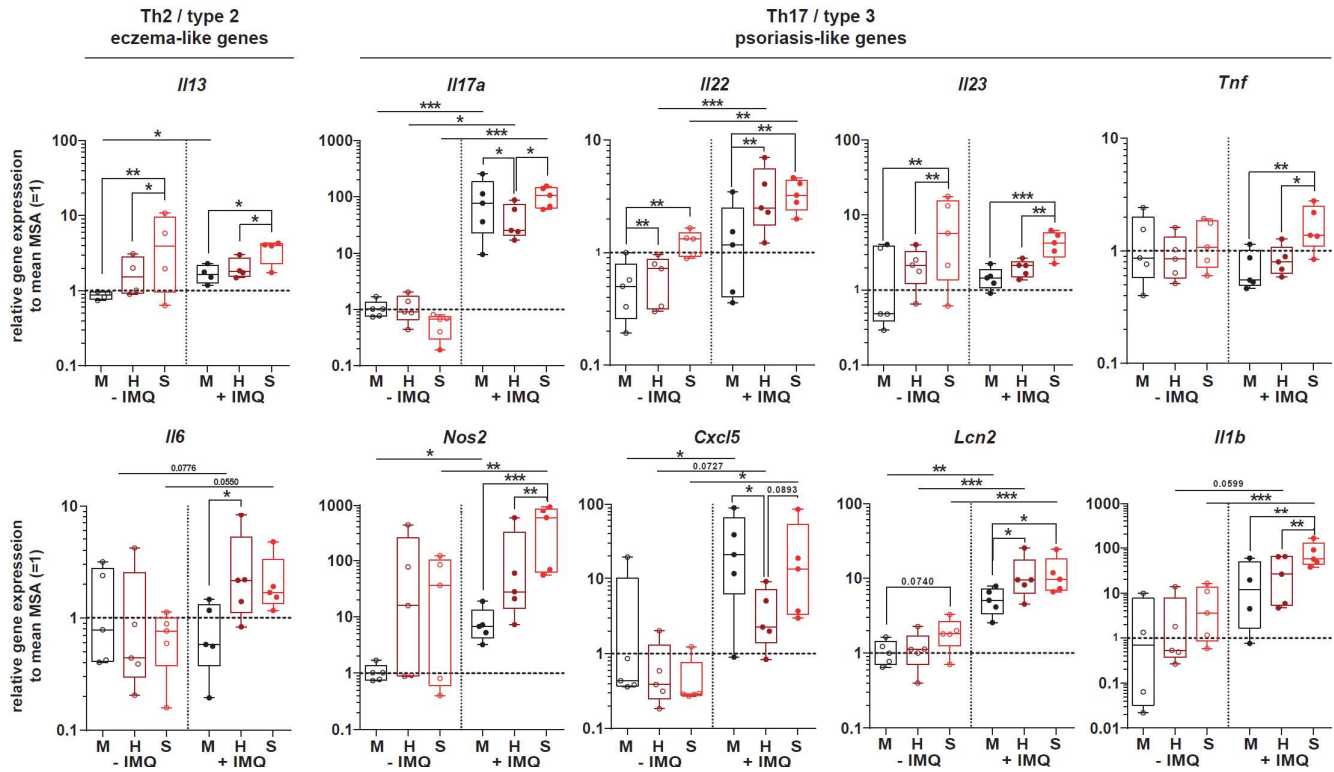


**Fig. S3: RNA expression of Th2/type 2 and Th17/type 3 disease marker genes in mice ears at day 6 after Serpinb3b (native (S) or heat-inactivated (H)/ MSA (M) injection and imiquimod (IMQ) application (n=5). Data were determined by qPCR. Relative gene expression was calculated to the mean MSA values of the – IMQ group using  $2^{\Delta\Delta ct}$  method and *Gapdh* as housekeeper. Comparison of injection types within – IMQ or + IMQ mouse groups was performed using ordinary one-way ANOVA test. Comparison of the injection type in – IMQ to + IMQ group was performed with an unpaired t-test. \* $p < 0.05$ , \*\* $p < 0.01$ , \*\*\* $p < 0.001$ , \*\*\*\* $p < 0.0001$ . M = MSA/murine serum albumin, H = heat-inactivated Serpinb3b, S = native Serpinb3b, IMQ = imiquimod.**

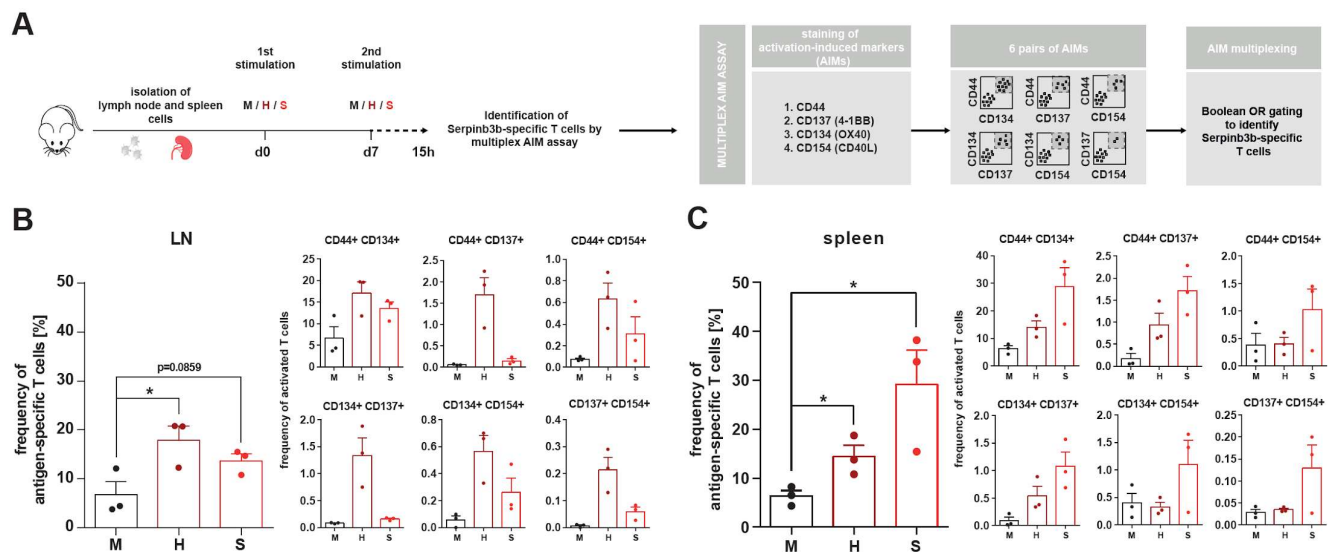


**Fig. S4: Wild-type mice possess a pool of Serpinb3b-reactive T cells.** The presence of Serpinb3b-reactive T cells in wild type mice was analyzed using the activation-induced markers (AIM) multiplex assay (82). **(A)** Study design: Lymph node cells and splenocytes from (n=5) wild-type mice were stimulated on day 0 and 7 *in vitro* with native (S) or heat-inactivated (H) Serpinb3b or with murine serum albumin (MSA) as control. 15 h after the second stimulation cells were analyzed by flow cytometry for the 4 activation-induced markers: CD44, CD137 (4-1BB), CD134 (OX40) and CD154 (CD40L), which identify antigen-specific T cells by Boolean OR gating of all six marker combinations. **(B&C)** The frequency of positive cells of the sum of all six marker combinations in lymph node cells (LN) (B) or splenocytes (C) corresponding to the frequency of Serpinb3b-reactive T cells is shown. Comparison of stimulation groups was performed using ordinary one-way ANOVA test. \* $p < 0.05$ , \*\* $p < 0.01$ , \*\*\* $p < 0.001$ , \*\*\*\* $p < 0.0001$ . S = native Serpinb3b, H = heat-inactivated Serpinb3b, MSA = murine serum albumin, AIM = activation-induced markers, LN = lymph nodes.

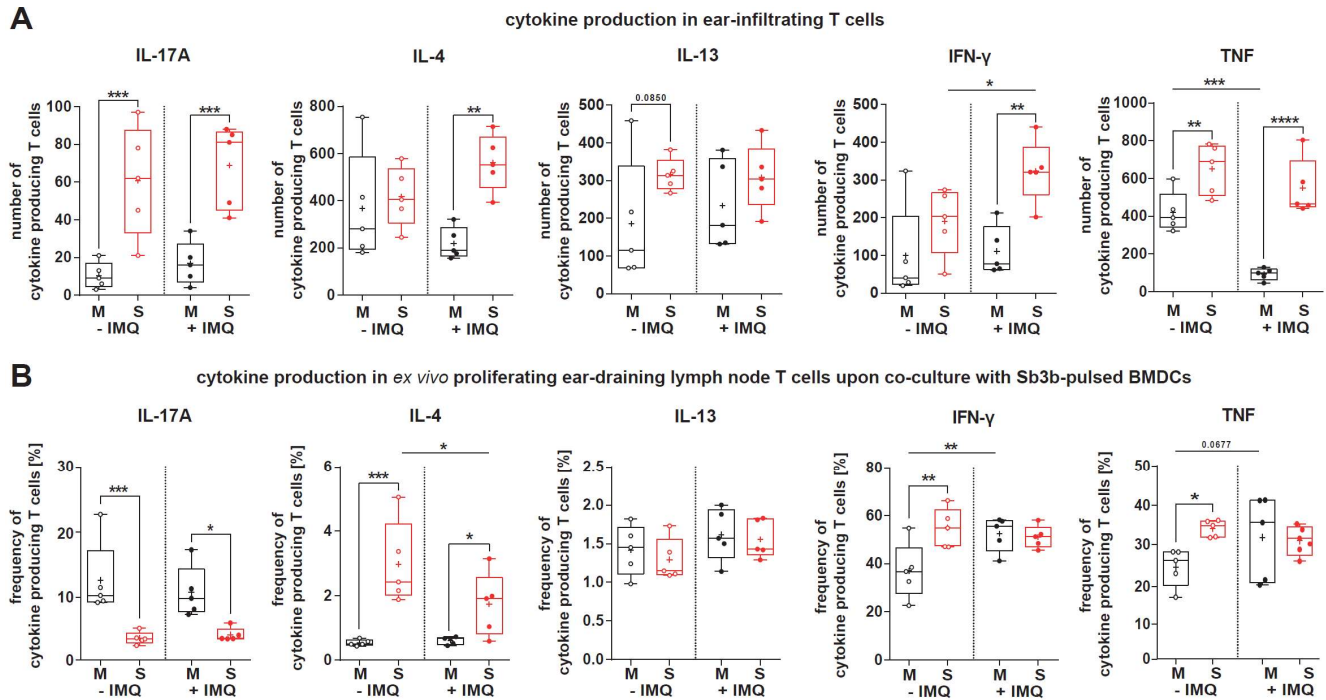


**Fig. S5: Cytokine profiles of ear-infiltrating T cells on day 18 (A) and *ex vivo* Serpinb3b proliferating ear-draining lymph node T cells on day 22 (B).** Cytokine production were determined by flow cytometry staining. Comparison within – IMQ or + IMQ mouse groups was performed using ordinary one-way ANOVA test. Comparison between the – IMQ to + IMQ groups was performed using unpaired t-test. \* $p < 0.05$ , \*\* $p < 0.01$ , \*\*\* $p < 0.001$ , \*\*\*\* $p < 0.0001$ . S = native Serpinb3b, M = murine serum albumin (MSA), IMQ = imiquimod.

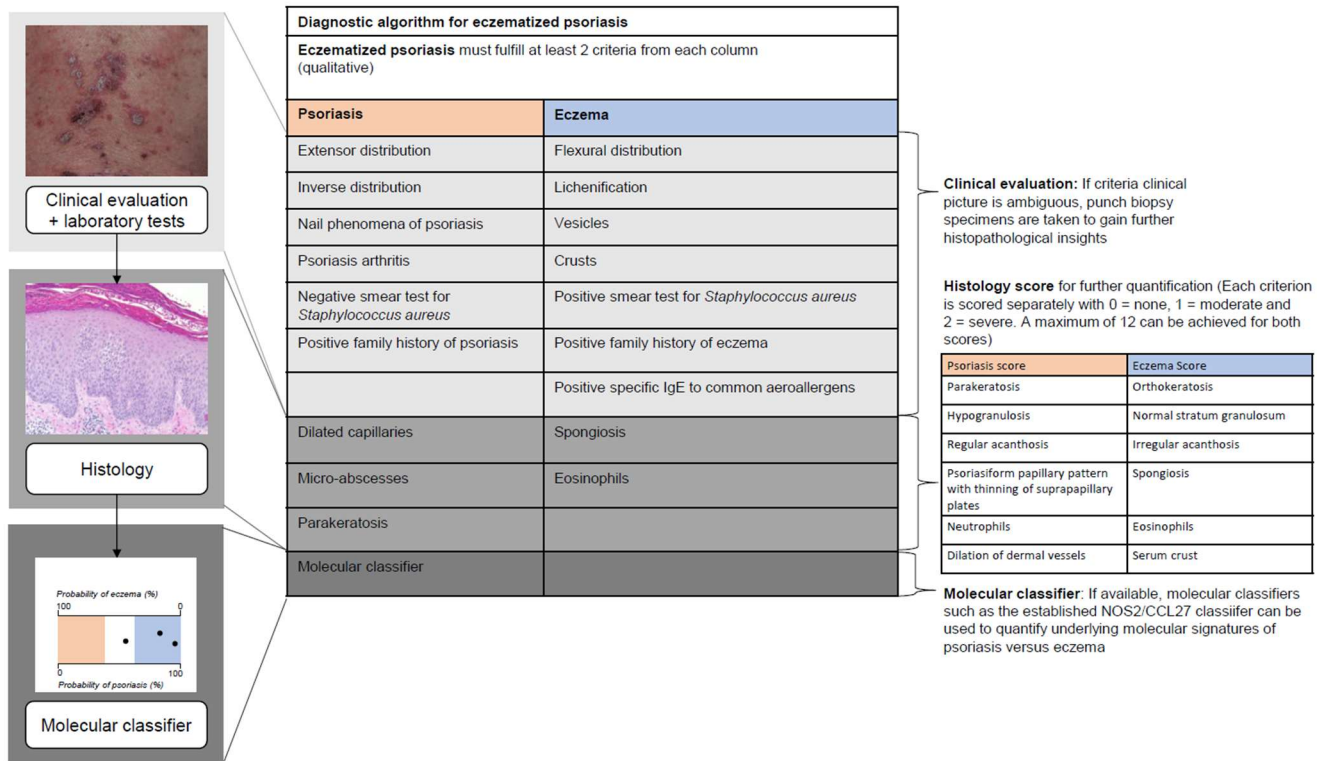


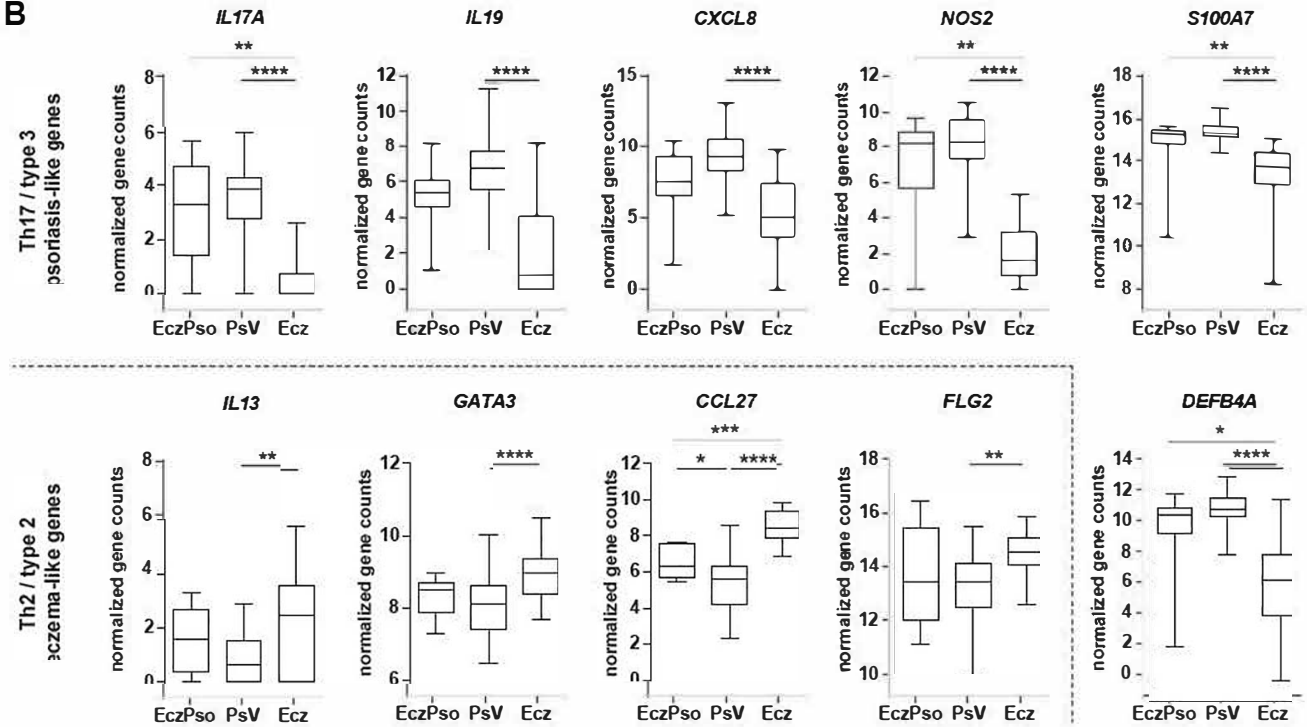
**Fig. S6. Workflow to the diagnosis of EczPso.**



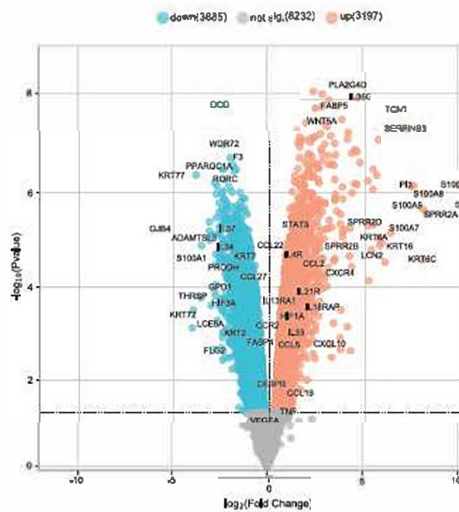
**A**



**B**



**C**



**D**

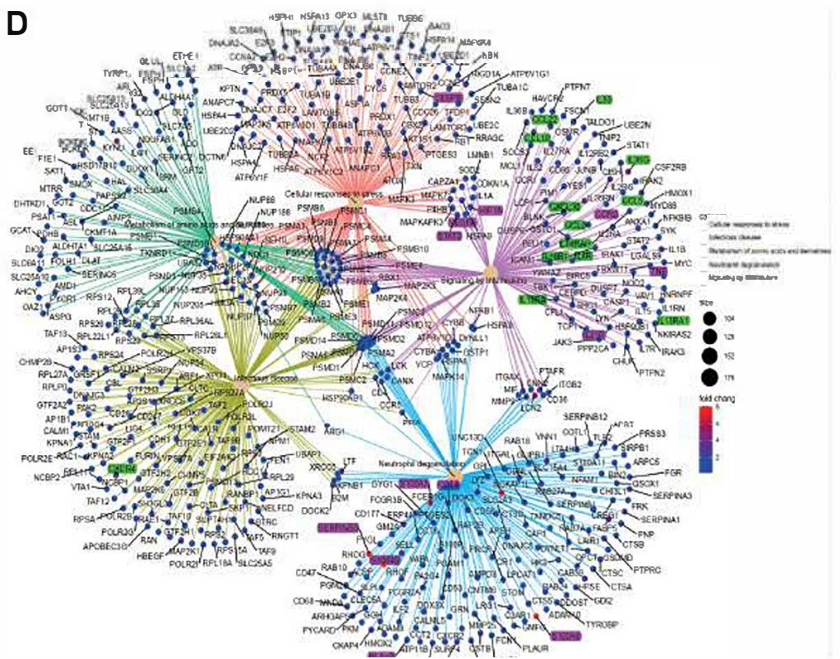


**Fig. S7: Histology and bulk RNAseq analysis of lesional skin demonstrates both Th2/type 2 and Th17/type 3 signatures in EczPso. (A)** Representative histological HE staining of lesional skin from EczPso, PsV and Ecz patients. Scale bar indicates 100  $\mu$ m. **(B-D)** Lesional and non-lesional skin of EczPso (n=9), PsV (n=34) and Ecz (n=20) patients was analyzed by bulk RNAseq. **(A)** Normalized gene counts of Th17/type 3 and Th2/type 2 signature genes within lesional skin of EczPso in comparison to PsV and Ecz patients. Ordinary one-way ANOVA test with Tukey's multiple comparison (for Gaussian distributed data) or nonparametric Kruskal-Wallis test with Dunn's multiple comparison (for non-Gaussian distributed data) was used to test for differences between disease groups. \* $p < 0.05$ , \*\* $p < 0.01$ , \*\*\* $p < 0.001$ , \*\*\*\* $p < 0.0001$ . **(C)** Volcano plot of differentially expressed genes between lesional and non-lesional (NL) skin of EczPso patients. **(B)** Reactome Pathway GSEA of log<sub>2</sub>FC ranked genes showed an upregulation of pathways associated with "Signaling by Interleukins", "Neutrophil degranulation", "Metabolism of amino acids and derivatives", "Infectious disease" and "Cellular responses to stress" in EczPso. Th2/type 2 (green) and Th17/type 3 (violet) signature genes are highlighted. EczPso = eczematized psoriasis, PsV = psoriasis vulgaris, Ecz = eczema, DEG = differentially expressed genes, GSEA = gene set enrichment analysis, FC = fold change, NL = non-lesional.

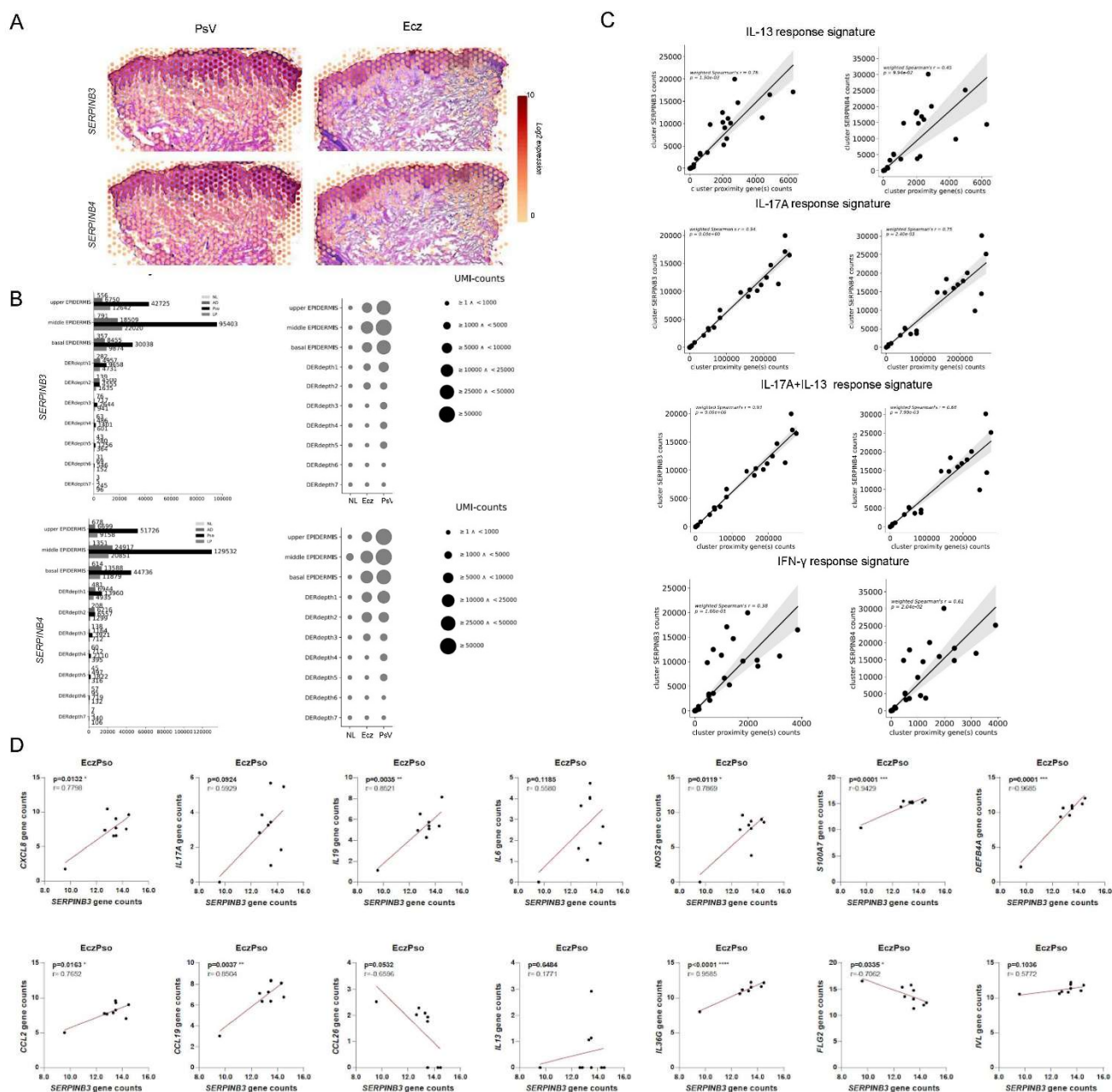


**Fig. S8. Spatial expression of SERPINB3 and SERPINB4 in the lesional skin. (A)** Representative spatial transcriptomics sections for PsV (n=9) and Ecz (n=9) with SERPINB3 and SERPINB4 transcript-positive spots ( $\varnothing 55 \mu\text{M}$ ). **(B)** Total UMI-counts of SERPINB3 within tissue layers of non-lesional (NL) skin, Ecz and PsV (left). UMI-counts of SERPINB3 in the manually annotated tissue layers in lesion and non-lesional skin (right). **(C)** Weighted Spearman correlation plots depicting the total expression levels of SERPINB3 and SERPINB4, respectively, along with their correlated *IL13*-induced, *IL17A*-induced, *IL13+IL17A*-induced and *IFNG*-induced responder signature genes within clusters at radius =

0 in lesion psoriatic skin biopsies. Statistical significance was estimated using a permutation-based p value approach for the weighted Spearman correlation. The regression line was fitted using an ordinary least squares (OLS) model, and the shaded area indicates the 95% confidence interval. Data and analysis method were originally published in Schäbitz et al. (83) and were reanalyzed here for the purpose of this method. **(D)** Spearman correlation scores of PsV and Ecz specific marker genes with SERPINB3 and SERPINB4 counts in EczPso patients. PsV = classical plaque-type psoriasis vulgaris, EczPso = eczematized psoriasis, Ecz = eczema, DER = Dermis, UMI = unique molecular identifiers.



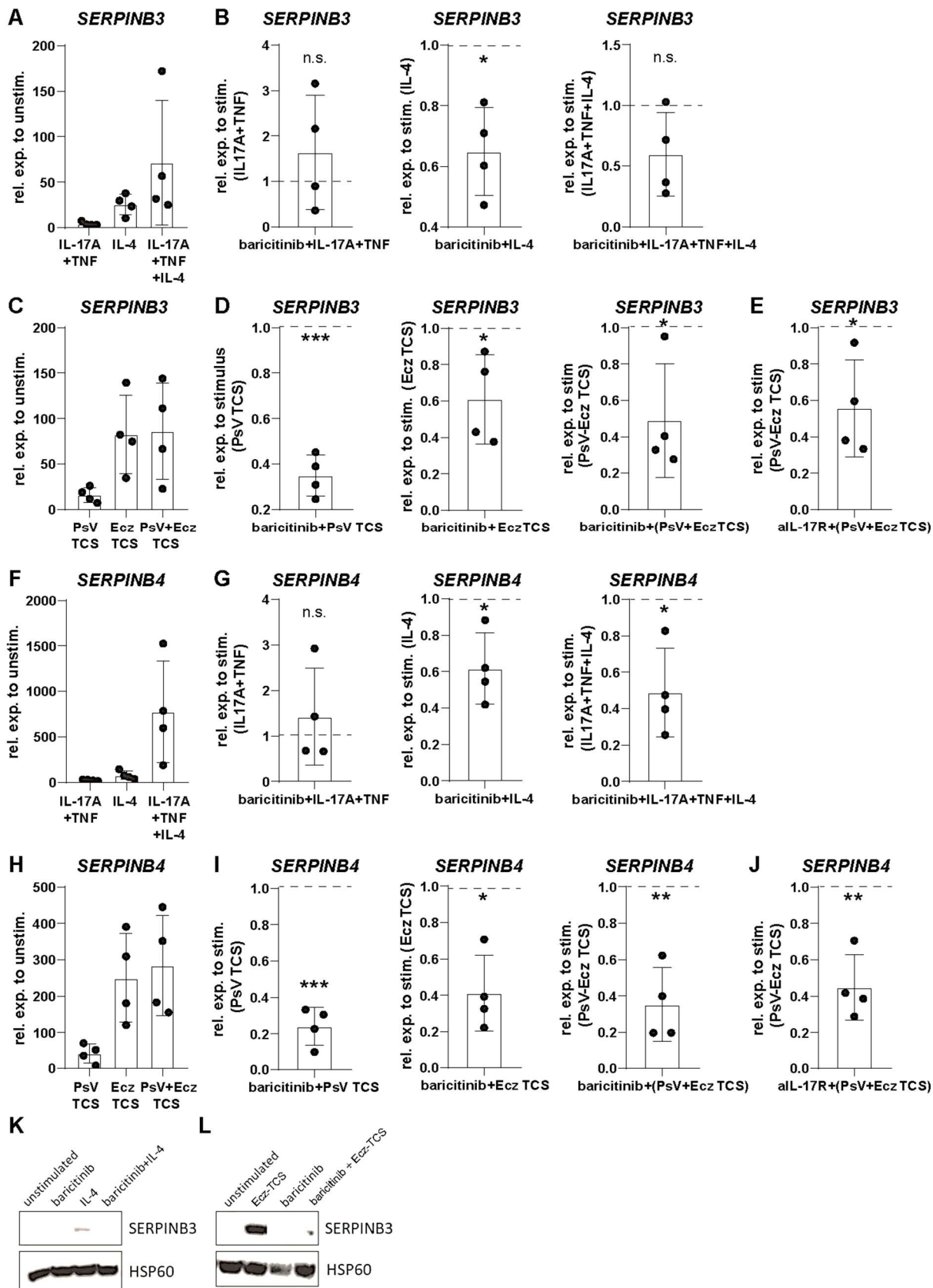


**Fig. S9. Therapeutic targeting of *SERPINB3* and *SERPINB4* expression.** *SERPINB3* expression in *in vitro* stimulated keratinocytes (n=4) analyzed with qPCR (**A-J**) and Western blot (**K-L**). Cells were stimulated for 16 h with IL-17A+TNF and/or IL-4 (A-B, F-G, K) or with lesional T cell supernatants isolated from PsV (n=4) or Ecz (n=3) skin biopsies (PsV and Ecz TCS were mixed 1:1 to generate PsV/Ecz TCS) (**C-E, H-J**) and pre-treated with 100 nM baricitinib (MedChemExpress, HY-15315) (**A-D, F-I, K-L**) or 2.5 µg/ml aIL-17 receptor inhibitor (R&D, #MAB177) (**E, J**) for one hour. Data are visualized as mean ± SD. Comparison to stimulated condition was performed using one sample t test for Gaussian distributed data, \*p<0.05, \*\*p<0.01, \*\*\*p<0.001. n.s. = not significant, PsV = classical plaque-type psoriasis vulgaris, Ecz = eczema, TCS = T cell supernatant.

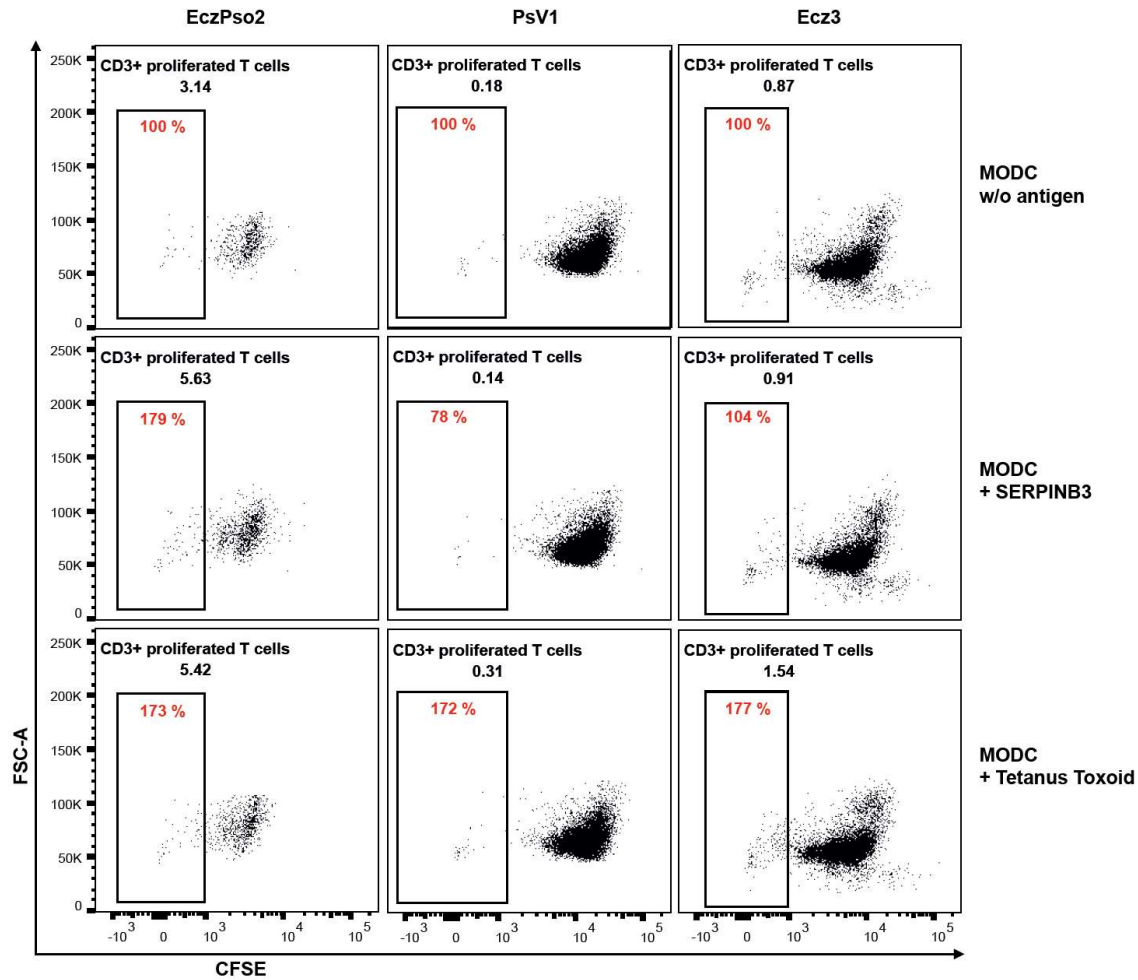


**Fig. S10: Representative CFSE tracings for lesional T cell proliferation assays upon SERPINB3 stimulation through MODCs.** Shown are lesional CFSE-stained T cells 10 d after co-culture with unstimulated (w/o antigen), SERPINB3 (10  $\mu$ g/ml) or tetanus toxoid (10  $\mu$ g/ml) stimulated MODCs for the patients EczPso2, PsV1 and Ecz3. Living CD3<sup>+</sup> T cells were gated and then presented as CFSE against FCS-A. Frequencies of CD3<sup>+</sup> proliferated T cells are indicated in black. Percentage of CD3<sup>+</sup> proliferated T cells compared to MODC control w/o antigen are highlighted in red. MODC = monocyte-derived dendritic cells, EczPso = eczematized psoriasis, PsV = classical plaque-type psoriasis vulgaris, Ecz = eczema.

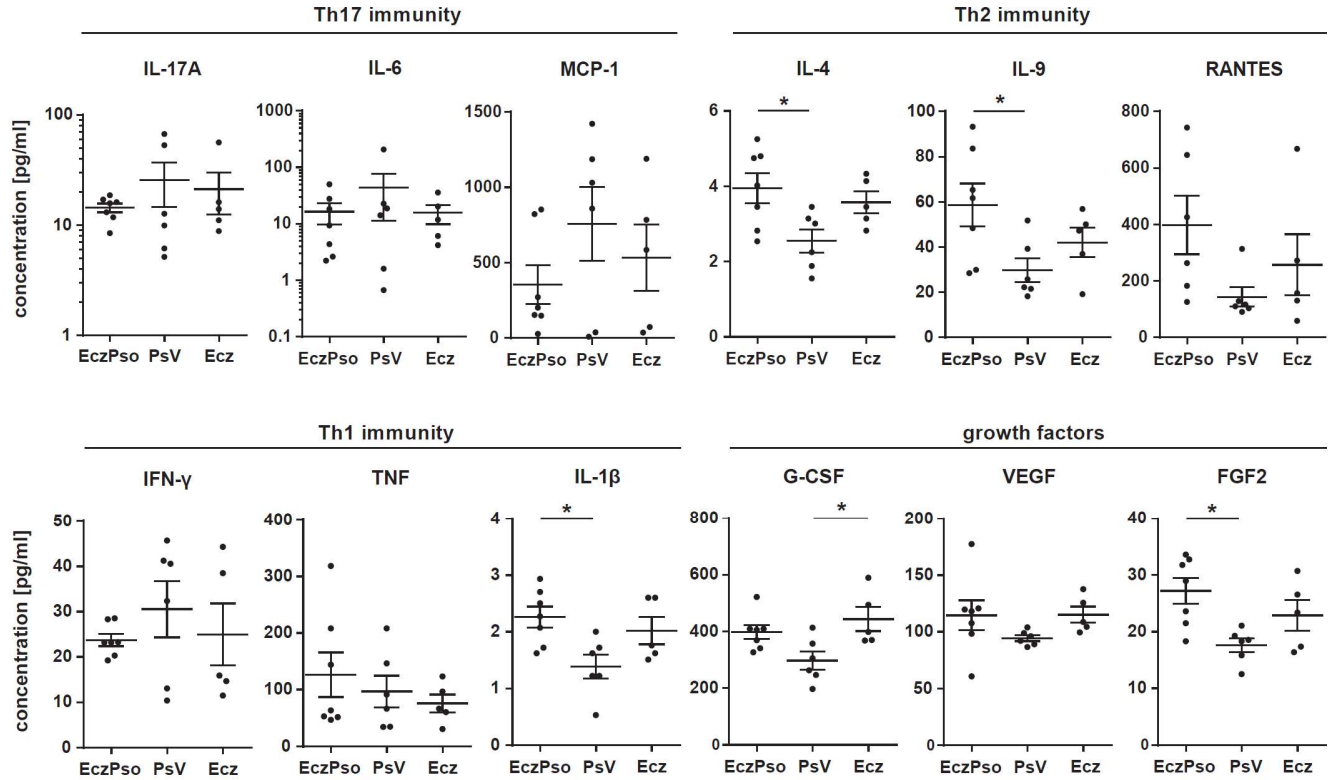


**Fig. S11: Lesional T cells of EczPso patients showed a predominant Th2 profile.** Cell-free supernatants derived from T cell proliferation assays from (Fig. 5C&D) were analyzed by multiplex assay and absolute concentrations are represented for Th17 (IL-17A, IL-6, MCP-1), Th2 (IL-4, IL-9, RANTES) and Th1 (IFN- $\gamma$ , TNF and IL-1 $\beta$ ) immunity proteins and growth factors (G-CSF, VEGF and FGF). Ordinary one-way ANOVA test with Tukey's multiple comparison was used to test for differences between disease groups. \*p<0.05. EczPso = eczematized psoriasis, PsV = psoriasis vulgaris, Ecz = eczema.

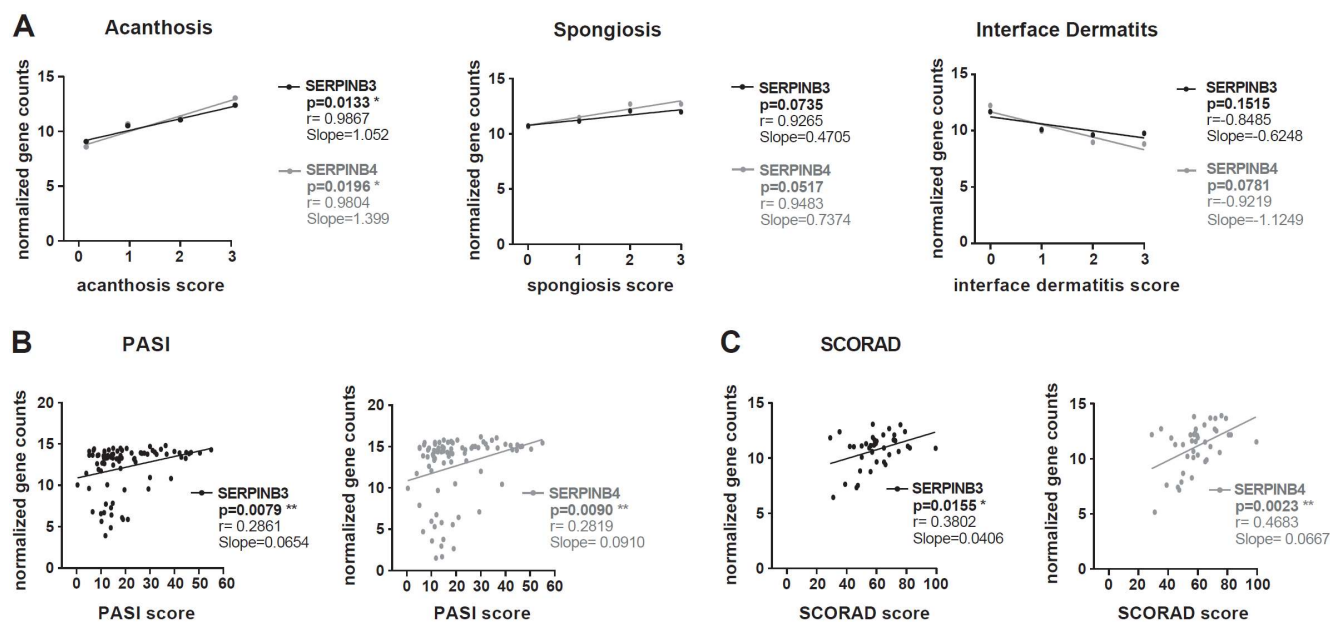


**Fig. S12: *SERPINB3* and *SERPINB4* gene expression correlates to clinical and histological features of EczPso.** (A) Correlation of histological patient scores for acanthosis, spongiosis and interface dermatitis severity to *SERPINB3* (black) and *SERPINB4* (grey) normalized gene counts from bulk RNAseq of lesional skin from ISD (n=261). Attribute scores were collected as ordinary data and classified as 0 (none), 1 (mild), 2 (moderate) or 3 (marked/severe). Plotted are the means of gene counts per attribute score level and their linear regression. (B&C) Correlation of *SERPINB3* (black) and *SERPINB4* (grey) normalized gene counts to PASI scores of PsV patients (top, n=85) (B) or SCORAD scores of Ecz patients (bottom, n=40) (C). Significance for linear regression was calculated by Pearson correlation. \*p<0.05, \*\*p<0.01. r = Pearson correlation score, PASI = Psoriasis Area and Severity Index, SCORAD = SCORing Atopic Dermatitis.

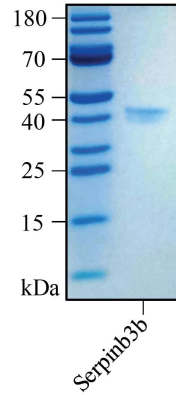


**Fig. S13: Purity assessment of recombinant Serpinb3b.** Reducing SDS-PAGE of purified, recombinant Serpinb3b in a 10 % Tris-Tricine gel including a pre-stained protein ladder (10-180 kDa) for molecular weight reference. Proteins were visualized by Coomassie brilliant blue staining. Densitometric analysis of the stained gel showed that the recombinant Serpinb3b has a purity of over 95 %.

## SUPPLEMENTARY TABLES

**Table S1. SERPINB3 and SERPINB4 peptide sequences.**

Sequence	Protein Accessions
FDQVTENTTGK	P29508
FDQVTENTTGKA	P29508
FDQVTENTTGKAATY	P29508
EYLDAIKKF	P29508;P48594
FIRQNKTNLSILFYGRFSSP	P29508;P48594
FLQEYLDAI	P29508;P48594
FQQFRKSKENNIF	P29508;P48594
FQQFRKSKENNIFYSPISIT	P29508;P48594
FQQFRKSKENNIFYSPISITSAL	P29508;P48594
FYGRFSSP	P29508;P48594
IVLLPNEIDGLQKLEEKL	P29508;P48594
IVLLPNEIDGLQKLEEKLTAEKL	P29508;P48594
KDTLRTMG	P29508;P48594
KSKENNIFYSPISITSALGMVL	P29508;P48594
LTEFNKSTDA	P29508;P48594
QEYLDAIKKF	P29508;P48594
SEANTKFMF	P29508;P48594
FDQVTENTTEK	P48594
LGAKDNTAQQISKVLHF	P48594
SSPSTNEEF	P48594
P29508: human SERPINB3, P48594: human SERPINB4	

**Table S2: Patient characteristics for the bulk RNA sequencing cohort of lesional skin from EczPso (n=9), PsV (n=34) and Ecz (n=20) patients.** Average values are shown as mean  $\pm$  standard error of mean (SEM). EczPso =eczematized psoriasis, PsV =classical plaque-type psoriasis vulgaris, Ecz = eczema, M = male, F = female, SEM = standard error of mean. Sequencing data can be obtained at GEO under the accession number GSE154200.

	Diagnosis_clinic	Diagnosis_histo	Seq_ID	Sex	Age
EczPso1	psoriasis vulgaris	eczematized psoriasis vulgaris	MUC7382	M	55
EczPso2	psoriasis vulgaris	eczematized psoriasis vulgaris	MUC7375	M	50
EczPso3	psoriasis vulgaris	eczematized psoriasis vulgaris	MUC7371	M	60
EczPso4	psoriasis vulgaris	eczematized psoriasis vulgaris	MUC7367	M	54
EczPso5	psoriasis vulgaris	eczematized psoriasis vulgaris	MUC7345	M	52
EczPso6	psoriasis vulgaris	eczematized psoriasis vulgaris	MUC7393	M	46
EczPso7	psoriasis vulgaris	eczematized psoriasis vulgaris	MUC7391	F	63
EczPso8	psoriasis vulgaris	eczematized psoriasis vulgaris	MUC7379	M	69

EczPso9	psoriasis vulgaris	eczematized psoriasis vulgaris	MUC7339	F	48
<b>Mean ± SEM (EczPso)</b>				<b>M:7 F:2</b>	<b>55 ± 2.5</b>
PsV1	psoriasis vulgaris	psoriasis vulgaris	MUC2737	F	18
PsV2	psoriasis vulgaris	psoriasis vulgaris	MUC2739	M	37
PsV3	psoriasis vulgaris	psoriasis vulgaris	MUC2741	M	45
PsV4	psoriasis vulgaris	psoriasis vulgaris	MUC2743	M	54
PsV5	psoriasis vulgaris	psoriasis vulgaris	MUC2745	M	33
PsV6	psoriasis vulgaris	psoriasis vulgaris	MUC2747	M	62
PsV7	psoriasis vulgaris	psoriasis vulgaris	MUC2751	M	47
PsV8	psoriasis vulgaris	psoriasis vulgaris	MUC2753	M	49
PsV9	psoriasis vulgaris	psoriasis vulgaris	MUC2757	F	38
PsV10	psoriasis vulgaris	psoriasis vulgaris	MUC2761	M	18
PsV11	psoriasis vulgaris	psoriasis vulgaris	MUC2763	F	65
PsV12	psoriasis vulgaris	psoriasis vulgaris	MUC2765	M	48
PsV13	psoriasis vulgaris	psoriasis vulgaris	MUC2771	F	27
PsV14	psoriasis vulgaris	psoriasis vulgaris	MUC2779	M	51
PsV15	psoriasis vulgaris	psoriasis vulgaris	MUC2781	F	49
PsV16	psoriasis vulgaris	psoriasis vulgaris	MUC2793	M	53
PsV17	psoriasis vulgaris	psoriasis vulgaris	MUC2803	F	41
PsV18	psoriasis vulgaris	psoriasis vulgaris	MUC4243	M	68
PsV19	psoriasis vulgaris	psoriasis vulgaris	MUC4245	M	43
PsV20	psoriasis vulgaris	psoriasis vulgaris	MUC4261	M	72
PsV21	psoriasis vulgaris	psoriasis vulgaris	MUC4267	M	76
PsV22	psoriasis vulgaris	psoriasis vulgaris	MUC4273	M	45
PsV23	psoriasis vulgaris	psoriasis vulgaris	MUC4293	M	32
PsV24	psoriasis vulgaris	psoriasis vulgaris	MUC4303	M	48
PsV25	psoriasis vulgaris	psoriasis vulgaris	MUC7329	M	46
PsV26	psoriasis vulgaris	psoriasis vulgaris	MUC7335	F	25
PsV27	psoriasis vulgaris	psoriasis vulgaris	MUC7337	M	25
PsV28	psoriasis vulgaris	psoriasis vulgaris	MUC7343	F	43
PsV29	psoriasis vulgaris	psoriasis vulgaris	MUC7349	F	60
PsV30	psoriasis vulgaris	psoriasis vulgaris	MUC7353	F	58
PsV31	psoriasis vulgaris	psoriasis vulgaris	MUC7355	M	68
PsV32	psoriasis vulgaris	psoriasis vulgaris	MUC7359	M	36
PsV33	psoriasis vulgaris	psoriasis vulgaris	MUC7361	M	67
PsV34	psoriasis vulgaris	psoriasis vulgaris	MUC7363	M	66
<b>Mean ± SEM (PsV)</b>				<b>M:24 F:10</b>	<b>47 ± 2.7</b>
Ecz1	eczema	eczema	MUC2678	M	22
Ecz2	eczema	eczema	MUC2680	F	17
Ecz3	eczema	eczema	MUC2684	M	18
Ecz4	eczema	eczema	MUC2690	M	62
Ecz5	eczema	eczema	MUC2697	F	75
Ecz6	eczema	eczema	MUC2703	F	31
Ecz7	eczema	eczema	MUC2707	M	58



Ecz8	eczema	eczema	MUC2711	M	25
Ecz9	eczema	eczema	MUC2717	M	21
Ecz10	eczema	eczema	MUC2945	M	76
Ecz11	eczema	eczema	MUC2951	M	66
Ecz12	eczema	eczema	MUC4279	M	37
Ecz13	eczema	eczema	MUC4281	M	75
Ecz14	eczema	eczema	MUC4285	M	59
Ecz15	eczema	eczema	MUC4287	M	21
Ecz16	eczema	eczema	MUC4291	M	50
Ecz17	eczema	eczema	MUC4301	M	55
Ecz18	eczema	eczema	MUC4313	M	73
Ecz19	eczema	eczema	MUC7333	F	21
Ecz20	eczema	eczema	MUC7320	F	23
<b>Mean ± SEM (Ecz)</b>				<b>M:15 F:5</b>	<b>44 ± 5.0</b>

**Table S3: Characteristics of healthy keratinocyte donors.** Average values are shown as mean  $\pm$  standard error of mean. M = male, F = female

Donor	Sex	Age	Diagnosis
D1	F	21.8	healthy
D2	M	52.1	healthy
D3	M	29.0	healthy
D4	M	22.3	healthy
n=4	F:1; M:3	31.3 $\pm$ 7.1	

**Table S4: Primer sequences**

Gene	species	Sequence (5'-3')	
<i>18S</i>	human	fw	GTA ACC CGT TGA ACC CCA TT
		rv	CCA TCC AAT CGG TAG TAG CG
<i>CCL27</i>	human	fw	CCC TAC AGC AGC ATT CCT AC
		rv	GTA GAG CTG AGT ACA GCA GGC
<i>NOS2</i>	human	fw	ATC TGC AGA CAC GTG CGT TA
		rv	TGA TGG CCG ACC TGA TGT TG
<i>SERPINB3</i>	human	fw	GGC AGC AAT ACC ACA TTG GTT C
		rv	GGA CTT GTA TGT ATT CTT GTT TGG C
<i>Cxcl5</i>	mouse	fw	TGC ATT CCG CTT AGC TTT CT
		rv	CAG AAG GAG GTC TGT CTG GA
<i>Gapdh</i>	mouse	rv	TTG ATG GCA ACA ATC TCC AC
		rv	CGT CCC GTA GAC AAA ATG
<i>Il1b</i>	mouse	fw	TTG TTG ATG TGC TGC TGT GA
		rv	TGT GAA ATG CCA CCT TTT GA
<i>Il6</i>	mouse	fw	ACC AGA GGA AAT TTT CAA TAG GC
		rv	TGA TGC ACT TGC AGA AAA CA
<i>Il13</i>	mouse	fw	ATG GCC TCT GTA ACC GCA AG
		rv	CTC ATT AGA AGG GGC CGT GG
<i>Il17a</i>	mouse	fw	TGA GCT TCC CAG ATC ACA GA
		rv	TCC AGA AGG CCC TCA GAC TA
<i>Il22</i>	mouse	fw	ATG AGT TTT TCC CTT ATG GGG AC
		rv	GCT GGA AGT TGG ACA CCT CAA
<i>Il23</i>	mouse	fw	GCT CCC CTT TGA AGA TGT CA

		rv	GAC CCA CAA GGA CTC AAG GA
<i>Lcn2</i>	mouse	fw	ACA TTT GTT CCA AGC TCC AGG GC
		rv	CAT GGC GAA CTG GTT GTA GTC CG
<i>Nos2</i>	mouse	fw	TCC AGG GAT TCT GGA ACA TT
		rv	GAA GAA AAC CCC TTG TGC TG
<i>Tnf</i>	mouse	fw	TC TAT GGC CCA GAC CCT CA
		rv	TGG TTT GCT ACG ACG TGG G

## SUPPLEMENTARY FILES

**Supplementary File 1:** List of HLA class I- and II-presented peptides identified in every sample analyzed by immunopeptidomics. Excel file.

**Supplementary File 2:** HLA Typing of MS cohort. Excel file.

## REFERENCES AND NOTES

1. P. Sewerin, R. Brinks, M. Schneider, I. Haase, S. Vordenbaumen, Prevalence and incidence of psoriasis and psoriatic arthritis. *Ann. Rheum. Dis.* **78**, 286–287 (2019).
2. R. Parisi, D. P. Symmons, C. E. Griffiths, D. M. Ashcroft, Identification and Management of Psoriasis Associated Comorbidity (IMPACT) project team, Global epidemiology of psoriasis: A systematic review of incidence and prevalence. *J. Invest. Dermatol.* **133**, 377–385 (2013).
3. E. Christophers, Explaining phenotype heterogeneity in patients with psoriasis. *Br. J. Dermatol.* **158**, 437–441 (2008).
4. A. R. Noorily, M. C. Criscito, J. M. Cohen, N. K. Brinster, Psoriasis with eczematous features: A retrospective clinicopathologic study. *Am. J. Dermatopathol.* **43**, 112–118 (2021).
5. C. E. M. Griffiths, A. W. Armstrong, J. E. Gudjonsson, J. Barker, Psoriasis. *Lancet* **397**, 1301–1315 (2021).
6. C. W. Lynde, Y. Poulin, R. Vender, M. Bourcier, S. Khalil, Interleukin 17A: Toward a new understanding of psoriasis pathogenesis. *J. Am. Acad. Dermatol.* **71**, 141–150 (2014).
7. A. Di Cesare, P. Di Meglio, F. O. Nestle, The IL-23/Th17 axis in the immunopathogenesis of psoriasis. *J. Invest. Dermatol.* **129**, 1339–1350 (2009).
8. A. Sharma, D. K. Upadhyay, G. D. Gupta, R. K. Narang, V. K. Rai, IL-23/Th17 axis: A potential therapeutic target of psoriasis. *Curr. Drug Res. Rev.* **14**, 24–36 (2022).
9. R. G. Langley, B. E. Elewski, M. Lebwohl, K. Reich, C. E. Griffiths, K. Papp, L. Puig, H. Nakagawa, L. Spelman, B. Sigurgeirsson, E. Rivas, T. F. Tsai, N. Wasel, S. Tying, T. Salko, I. Hampele, M. Notter, A. Karpov, S. Helou, C. Papavassilis, ERASURE Study Group, FIXTURE Study Group, Secukinumab in plaque psoriasis—Results of two phase 3 trials. *N. Engl. J. Med.* **371**, 326–338 (2014).

10. C. Leonardi, R. Matheson, C. Zachariae, G. Cameron, L. Li, E. Edson-Heredia, D. Braun, S. Banerjee, Anti-interleukin-17 monoclonal antibody ixekizumab in chronic plaque psoriasis. *N. Engl. J. Med.* **366**, 1190–1199 (2012).
11. K. A. Papp, J. F. Merola, A. B. Gottlieb, C. E. M. Griffiths, N. Cross, L. Peterson, C. Cioffi, A. Blauvelt, Dual neutralization of both interleukin 17A and interleukin 17F with bimekizumab in patients with psoriasis: Results from BE ABLE 1, a 12-week randomized, double-blinded, placebo-controlled phase 2b trial. *J. Am. Acad. Dermatol.* **79**, 277–286.e10 (2018).
12. K. A. Papp, C. Leonardi, A. Menter, J. P. Ortonne, J. G. Krueger, G. Kricorian, G. Aras, J. Li, C. B. Russell, E. H. Thompson, S. Baumgartner, Brodalumab, an anti-interleukin-17-receptor antibody for psoriasis. *N. Engl. J. Med.* **366**, 1181–1189 (2012).
13. R. P. Nair, P. E. Stuart, I. Nistor, R. Hiremagalore, N. V. C. Chia, S. Jenisch, M. Weichenthal, G. R. Abecasis, H. W. Lim, E. Christophers, J. J. Voorhees, J. T. Elder, Sequence and haplotype analysis supports HLA-C as the psoriasis susceptibility 1 gene. *Am. J. Hum. Genet.* **78**, 827–851 (2006).
14. Z. Shen, G. Wang, J. Y. Fan, W. Li, Y. F. Liu, HLA DR B1\*04, \*07-restricted epitopes on keratin 17 for autoreactive T cells in psoriasis. *J. Dermatol. Sci.* **38**, 25–39 (2005).
15. R. Lande, E. Botti, C. Jandus, D. Dojcinovic, G. Fanelli, C. Conrad, G. Chamilos, L. Feldmeyer, B. Marinari, S. Chon, L. Vence, V. Riccieri, P. Guillaume, A. A. Navarini, P. Romero, A. Costanzo, E. Piccolella, M. Gilliet, L. Frasca, The antimicrobial peptide LL37 is a T-cell autoantigen in psoriasis. *Nat. Commun.* **5**, 5621 (2014).
16. A. Arakawa, K. Siewert, J. Stohr, P. Besgen, S. M. Kim, G. Ruhl, J. Nickel, S. Vollmer, P. Thomas, S. Krebs, S. Pinkert, M. Spannagl, K. Held, C. Kammerbauer, R. Besch, K. Dornmair, J. C. Prinz, Melanocyte antigen triggers autoimmunity in human psoriasis. *J. Exp. Med.* **212**, 2203–2212 (2015).

17. S. Nishimoto, H. Kotani, S. Tsuruta, N. Shimizu, M. Ito, T. Shichita, R. Morita, H. Takahashi, M. Amagai, A. Yoshimura, Th17 cells carrying TCR recognizing epidermal autoantigen induce psoriasis-like skin inflammation. *J. Immunol.* **191**, 3065–3072 (2013).
18. O. J. Iversen, H. Lysvand, G. Slupphaug, Pso p27, a SERPINB3/B4-derived protein, is most likely a common autoantigen in chronic inflammatory diseases. *Clin. Immunol.* **174**, 10–17 (2017).
19. K. L. Cheung, R. Jarrett, S. Subramaniam, M. Salimi, D. Gutowska-Owsiak, Y. L. Chen, C. Hardman, L. Xue, V. Cerundolo, G. Ogg, Psoriatic T cells recognize neolipid antigens generated by mast cell phospholipase delivered by exosomes and presented by CD1a. *J. Exp. Med.* **213**, 2399–2412 (2016).
20. O. Rotzschke, K. Falk, H. J. Wallny, S. Faath, H. G. Rammensee, Characterization of naturally occurring minor histocompatibility peptides including H-4 and H-Y. *Science* **249**, 283–287 (1990).
21. J. G. Abelin, E. J. Bergstrom, K. D. Rivera, H. B. Taylor, S. Klaeger, C. Xu, E. K. Verzani, C. Jackson White, H. B. Woldemichael, M. Virshup, M. E. Olive, M. Maynard, S. A. Vartany, J. D. Allen, K. Phulphagar, M. Harry Kane, S. Rachimi, D. R. Mani, M. A. Gillette, S. Satpathy, K. R. Clauser, N. D. Udeshi, S. A. Carr, Workflow enabling deepscale immunopeptidome, proteome, ubiquitylome, phosphoproteome, and acetylome analyses of sample-limited tissues. *Nat. Commun.* **14**, 1851 (2023).
22. L. K. Freudenmann, A. Marcu, S. Stevanovic, Mapping the tumour human leukocyte antigen (HLA) ligandome by mass spectrometry. *Immunology* **154**, 331–345 (2018).
23. A. M. Jaeger, L. E. Stopfer, R. Ahn, E. A. Sanders, D. A. Sandel, W. A. Freed-Pastor, W. M. Rideout III, S. Naranjo, T. Fessenden, K. B. Nguyen, P. S. Winter, R. E. Kohn, P. M. K. Westcott, J. M. Schenkel, S. L. Shanahan, A. K. Shalek, S. Spranger, F. M. White, T. Jacks, Deciphering the immunopeptidome in vivo reveals new tumour antigens. *Nature* **607**, 149–155 (2022).

24. Y. Sun, N. Sheshadri, W. X. Zong, SERPINB3 and B4: From biochemistry to biology. *Semin. Cell Dev. Biol.* **62**, 170–177 (2017).
25. U. Sivaprasad, D. J. Askew, M. B. Ericksen, A. M. Gibson, M. T. Stier, E. B. Brandt, S. A. Bass, M. O. Daines, J. Chakir, K. F. Stringer, S. E. Wert, J. A. Whitsett, T. D. Le Cras, M. Wills-Karp, G. A. Silverman, G. K. Khurana Hershey, A nonredundant role for mouse Serpinb3a in the induction of mucus production in asthma. *J. Allergy Clin. Immunol.* **127**, 254–261.e6 (2011).
26. R. M. Chicz, R. G. Urban, J. C. Gorga, D. A. Vignali, W. S. Lane, J. L. Strominger, Specificity and promiscuity among naturally processed peptides bound to HLA-DR alleles. *J. Exp. Med.* **178**, 27–47 (1993).
27. O. Rotzschke, K. Falk, Origin, structure and motifs of naturally processed MHC class II ligands. *Curr. Opin. Immunol.* **6**, 45–51 (1994).
28. F. Sinigaglia, J. Hammer, Defining rules for the peptide-MHC class II interaction. *Curr. Opin. Immunol.* **6**, 52–56 (1994).
29. S. Costa, D. Bevilacqua, E. Cavegion, S. Gasperini, E. Zenaro, F. Pettinella, M. Donini, S. Dusi, G. Constantin, S. Lonardi, W. Vermi, F. De Sanctis, S. Ugel, T. Cestari, C. L. Abram, C. A. Lowell, P. Rodegher, F. Tagliaro, G. Girolomoni, M. A. Cassatella, P. Scapini, Neutrophils inhibit gammadelta T cell functions in the imiquimod-induced mouse model of psoriasis. *Front. Immunol.* **13**, 1049079 (2022).
30. F. Li, D. Han, B. Wang, W. Zhang, Y. Zhao, J. Xu, L. Meng, K. Mou, S. Lu, W. Zhu, Y. Zhou, Topical treatment of colquhounia root relieves skin inflammation and itch in imiquimod-induced psoriasiform dermatitis in mice. *Mediators Inflamm.* **2022**, 5782922 (2022).
31. L. van der Fits, S. Mourits, J. S. Voerman, M. Kant, L. Boon, J. D. Laman, F. Cornelissen, A. M. Mus, E. Florencia, E. P. Prens, E. Lubberts, Imiquimod-induced psoriasis-like skin inflammation in mice is mediated via the IL-23/IL-17 axis. *J. Immunol.* **182**, 5836–5845 (2009).

32. F. Lauffer, K. Eyerich, Eczematized psoriasis—A frequent but often neglected variant of plaque psoriasis. *J. Dtsch. Dermatol. Ges.* **21**, 445–453 (2023).
33. H. Vinter, L. Iversen, T. Steiniche, K. Kragballe, C. Johansen, Aldara(R)-induced skin inflammation: Studies of patients with psoriasis. *Br. J. Dermatol.* **172**, 345–353 (2015).
34. N. Garzorz-Stark, F. Lauffer, L. Krause, J. Thomas, A. Atenhan, R. Franz, S. Roenneberg, A. Boehner, M. Jargosch, R. Batra, N. S. Mueller, S. Haak, C. Gross, O. Gross, C. Traidl-Hoffmann, F. J. Theis, C. B. Schmidt-Weber, T. Biedermann, S. Eyerich, K. Eyerich, Toll-like receptor 7/8 agonists stimulate plasmacytoid dendritic cells to initiate TH17-deviated acute contact dermatitis in human subjects. *J. Allergy Clin. Immunol.* **141**, 1320–1333.e11 (2018).
35. A. Al-Janabi, A. C. Foulkes, C. E. M. Griffiths, R. B. Warren, Paradoxical eczema in patients with psoriasis receiving biologics: A case series. *Clin. Exp. Dermatol.* **47**, 1174–1178 (2022).
36. Y. Zhang, G. Jiang, Application of JAK inhibitors in paradoxical reaction through immune-related dermatoses. *Front. Immunol.* **15**, 1341632 (2024).
37. N. Garzorz-Stark, L. Krause, F. Lauffer, A. Atenhan, J. Thomas, S. P. Stark, R. Franz, S. Weidinger, A. Balato, N. S. Mueller, F. J. Theis, J. Ring, C. B. Schmidt-Weber, T. Biedermann, S. Eyerich, K. Eyerich, A novel molecular disease classifier for psoriasis and eczema. *Exp. Dermatol.* **25**, 767–774 (2016).
38. M. Bassani-Sternberg, E. Braunlein, R. Klar, T. Engleitner, P. Sinitcyn, S. Audehm, M. Straub, J. Weber, J. Slotta-Huspenina, K. Specht, M. E. Martignoni, A. Werner, R. Hein, D. H. Busch, C. Peschel, R. Rad, J. Cox, M. Mann, A. M. Krackhardt, Direct identification of clinically relevant neoepitopes presented on native human melanoma tissue by mass spectrometry. *Nat. Commun.* **7**, 13404 (2016).
39. A. Marcu, L. Bichmann, L. Kuchenbecker, D. J. Kowalewski, L. K. Freudenmann, L. Backert, L. Muhlenbruch, A. Szolek, M. Lubke, P. Wagner, T. Engler, S. Matovina, J. Wang, M. Hauri-Hohl, R. Martin, K. Kapolou, J. S. Walz, J. Velz, H. Moch, L. Regli, M. Silginer, M. Weller, M. W. Loffler, F. Erhard, A. Schlosser, O. Kohlbacher, S. Stevanovic, H. G.



- Rammensee, M. C. Neidert, HLA ligand atlas: A benign reference of HLA-presented peptides to improve T-cell-based cancer immunotherapy. *J. Immunother. Cancer* **9**, eabn9644 (2021).
40. C. R. Parish, Cancer immunotherapy: The past, the present and the future. *Immunol. Cell Biol.* **81**, 106–113 (2003).
41. V. Velcheti, K. Schalper, Basic overview of current immunotherapy approaches in cancer. *Am. Soc. Clin. Oncol. Educ. Book* **35**, 298–308 (2016).
42. M. Y. Mapara, M. Sykes, Tolerance and cancer: Mechanisms of tumor evasion and strategies for breaking tolerance. *J. Clin. Oncol.* **22**, 1136–1151 (2004).
43. D. Mougiakakos, G. Kronke, S. Volkl, S. Kretschmann, M. Aigner, S. Kharboutli, S. Boltz, B. Manger, A. Mackensen, G. Schett, CD19-targeted CAR T cells in refractory systemic lupus erythematosus. *N. Engl. J. Med.* **385**, 567–569 (2021).
44. C. Krienke, L. Kolb, E. Diken, M. Streuber, S. Kirchhoff, T. Bukur, O. Akilli-Ozturk, L. M. Kranz, H. Berger, J. Petschenka, M. Diken, S. Kreiter, N. Yogeve, A. Waisman, K. Kariko, O. Tureci, U. Sahin, A noninflammatory mRNA vaccine for treatment of experimental autoimmune encephalomyelitis. *Science* **371**, 145–153 (2021).
45. J. G. Krueger, An autoimmune “attack” on melanocytes triggers psoriasis and cellular hyperplasia. *J. Exp. Med.* **212**, 2186 (2015).
46. A. Takeda, D. Higuchi, T. Takahashi, M. Ogo, P. Baci, P. F. Goetinck, T. Hibino, Overexpression of serpin squamous cell carcinoma antigens in psoriatic skin. *J. Invest. Dermatol.* **118**, 147–154 (2002).
47. J. Fuentes-Duculan, K. M. Bonifacio, J. E. Hawkes, N. Kunjraiva, I. Cueto, X. Li, J. Gonzalez, S. Garcet, J. G. Krueger, Autoantigens ADAMTSL5 and LL37 are significantly upregulated in active psoriasis and localized with keratinocytes, dendritic cells and other leukocytes. *Exp. Dermatol.* **26**, 1075–1082 (2017).

48. M. Bassani-Sternberg, S. Pletscher-Frankild, L. J. Jensen, M. Mann, Mass spectrometry of human leukocyte antigen class I peptidomes reveals strong effects of protein abundance and turnover on antigen presentation. *Mol. Cell. Proteomics* **14**, 658–673 (2015).
49. F. Numa, O. Takeda, M. Nakata, S. Nawata, N. Tsunaga, K. Hirabayashi, Y. Suminami, H. Kato, S. Hamanaka, Tumor necrosis factor- $\alpha$  stimulates the production of squamous cell carcinoma antigen in normal squamous cells. *Tumour Biol.* **17**, 97–101 (1996).
50. Y. Uemura, S. C. Pak, C. Luke, S. Cataltepe, C. Tsu, C. Schick, Y. Kamachi, S. L. Pomeroy, D. H. Perlmutter, G. A. Silverman, Circulating serpin tumor markers SCCA1 and SCCA2 are not actively secreted but reside in the cytosol of squamous carcinoma cells. *Int. J. Cancer* **89**, 368–377 (2000).
51. A. Schabitz, C. Hillig, M. Mubarak, M. Jargosch, A. Farnoud, E. Scala, N. Kurzen, A. C. Pilz, N. Bhalla, J. Thomas, M. Stahle, T. Biedermann, C. B. Schmidt-Weber, F. Theis, N. Garzorz-Stark, K. Eyerich, M. P. Menden, S. Eyerich, Spatial transcriptomics landscape of lesions from non-communicable inflammatory skin diseases. *Nat. Commun.* **13**, 7729 (2022).
52. H. Maciejewska-Rodrigues, M. Al-Shamisi, H. Hemmatazad, C. Ospelt, M. C. Bouton, D. Jager, A. P. Cope, P. Charles, D. Plant, J. H. Distler, R. E. Gay, B. A. Michel, A. Knuth, M. Neidhart, S. Gay, A. Jungel, Functional autoantibodies against serpin E2 in rheumatoid arthritis. *Arthritis Rheum.* **62**, 93–104 (2010).
53. Y. Kryvalap, M. L. Jiang, N. Kryvalap, C. Hendrickson, J. Czyzyk, SerpinB13 antibodies promote  $\beta$  cell development and resistance to type 1 diabetes. *Sci. Transl. Med.* **13**, eabf1587 (2021).
54. M. Gatto, L. Iaccarino, A. Ghirardello, N. Bassi, P. Pontisso, L. Punzi, Y. Shoenfeld, A. Doria, Serpins, immunity and autoimmunity: Old molecules, new functions. *Clin Rev Allergy Immunol* **45**, 267–280 (2013).
55. H. Lysvand, R. Helland, L. Hagen, G. Slupphaug, O. J. Iversen, Psoriasis pathogenesis—Pso p27 constitutes a compact structure forming large aggregates. *Biochem. Biophys. Rep.* **2**, 132–136 (2015).

56. H. Lysvand, L. Hagen, L. Klubicka, G. Slupphaug, O. J. Iversen, Psoriasis pathogenesis—Pso p27 is generated from SCCA1 with chymase. *Biochim. Biophys. Acta* **1842**, 734–738 (2014).
57. Y. Nagata, R. Suzuki, FcεRI: A master regulator of mast cell functions. *Cells* **11**, 622 (2022).
58. K. Mukai, M. Tsai, H. Saito, S. J. Galli, Mast cells as sources of cytokines, chemokines, and growth factors. *Immunol. Rev.* **282**, 121–150 (2018).
59. D. Simon, E. Vassina, S. Yousefi, E. Kozlowski, L. R. Braathen, H. U. Simon, Reduced dermal infiltration of cytokine-expressing inflammatory cells in atopic dermatitis after short-term topical tacrolimus treatment. *J. Allergy Clin. Immunol.* **114**, 887–895 (2004).
60. W. Xiao, K. Sha, M. Wang, Z. Tan, Y. Wang, S. Xu, Z. Zhao, Q. Wang, H. Xie, M. Chen, Z. Deng, J. Li, SERPINB3/B4 is increased in psoriasis and rosacea lesions and has proinflammatory effects in mouse models of these diseases. *J. Invest. Dermatol.* **144**, 2706–2718.e6 (2024).
61. T. R. Matos, J. T. O'Malley, E. L. Lowry, D. Hamm, I. R. Kirsch, H. S. Robins, T. S. Kupper, J. G. Krueger, R. A. Clark, Clinically resolved psoriatic lesions contain psoriasis-specific IL-17-producing alphabeta T cell clones. *J. Clin. Invest.* **127**, 4031–4041 (2017).
62. S. M. Lwin, J. A. Snowden, C. E. M. Griffiths, The promise and challenges of cell therapy for psoriasis. *Br. J. Dermatol.* **185**, 887–898 (2021).
63. K. Schakel, K. Reich, K. Asadullah, A. Pinter, D. Jullien, P. Weisenseel, C. Paul, M. Gomez, S. Wegner, Y. Personke, F. Kreimendahl, Y. Chen, J. Angsana, M. W. L. Leung, K. Eyerich, Early disease intervention with guselkumab in psoriasis leads to a higher rate of stable complete skin clearance ('clinical super response'): Week 28 results from the ongoing phase IIIb randomized, double-blind, parallel-group, GUIDE study. *J. Eur. Acad. Dermatol. Venereol.* **37**, 2016–2027 (2023).

64. L. Iversen, C. Conrad, L. Eidsmo, A. Costanzo, J. Narbutt, A. Pinter, K. Kingo, R. Rivera Diaz, F. Kolbinger, M. Nanna, J. A. Frueh, P. Jagiello, Secukinumab demonstrates superiority over narrow-band ultraviolet B phototherapy in new-onset moderate to severe plaque psoriasis patients: Week 52 results from the STEPIn study. *J. Eur. Acad. Dermatol. Venereol.* **37**, 1004–1016 (2023).
65. D. J. Kowalewski, S. Stevanovic, Biochemical large-scale identification of MHC class I ligands. *Methods Mol. Biol.* **960**, 145–157 (2013).
66. C. J. Barnstable, W. F. Bodmer, G. Brown, G. Galfre, C. Milstein, A. F. Williams, A. Ziegler, Production of monoclonal antibodies to group A erythrocytes, HLA and other human cell surface antigens-new tools for genetic analysis. *Cell* **14**, 9–20 (1978).
67. G. Pawelec, A. Ziegler, P. Wernet, Dissection of human allostimulatory determinants with cloned T cells: Stimulation inhibition by monoclonal antibodies TU22, 34, 35, 36, 37, 39, 43, and 58 against distinct human MHC class II molecules. *Hum. Immunol.* **12**, 165–176 (1985).
68. J. M. Goldman, J. Hibbin, L. Kearney, K. Orchard, K. H. Th'ng, HLA-DR monoclonal antibodies inhibit the proliferation of normal and chronic granulocytic leukaemia myeloid progenitor cells. *Br. J. Haematol.* **52**, 411–420 (1982).
69. D. J. Kowalewski, H. Schuster, L. Backert, C. Berlin, S. Kahn, L. Kanz, H. R. Salih, H. G. Rammensee, S. Stevanovic, J. S. Stickel, HLA ligandome analysis identifies the underlying specificities of spontaneous antileukemia immune responses in chronic lymphocytic leukemia (CLL). *Proc. Natl. Acad. Sci. U.S.A.* **112**, E166–E175 (2015).
70. J. K. Eng, A. L. McCormack, J. R. Yates, An approach to correlate tandem mass spectral data of peptides with amino acid sequences in a protein database. *J. Am. Soc. Mass Spectrom.* **5**, 976–989 (1994).
71. P. Speth, M. Jargosch, P. Seiringer, K. Schwamborn, T. Bauer, C. Scheerer, U. Protzer, C. Schmidt-Weber, T. Biedermann, S. Eyerich, N. Garzorz-Stark, Immunocompromised patients with therapy-refractory chronic skin diseases show reactivation of latent Epstein–Barr virus and cytomegalovirus infection. *J. Invest. Dermatol.* **142**, 549–558.e6 (2022).

72. F. Lauffer, M. Jargosch, L. Krause, N. Garzorz-Stark, R. Franz, S. Roenneberg, A. Bohner, N. S. Mueller, F. J. Theis, C. B. Schmidt-Weber, T. Biedermann, S. Eyerich, K. Eyerich, Type I immune response induces keratinocyte necroptosis and is associated with interface dermatitis. *J. Invest. Dermatol.* **138**, 1785–1794 (2018).
73. Z. Kurgys, L. Vornholz, K. Pechloff, L. V. Kemeny, T. Wartewig, A. Muschaweckh, A. Joshi, K. Kranen, L. Hartjes, S. Mockel, K. Steiger, E. Hameister, T. Volz, M. Mellett, L. E. French, T. Biedermann, T. Korn, J. Ruland, Keratinocyte-intrinsic BCL10/MALT1 activity initiates and amplifies psoriasiform skin inflammation. *Sci. Immunol.* **6**, eabi4425 (2021).
74. T. Sparwasser, R. M. Vabulas, B. Villmow, G. B. Lipford, H. Wagner, Bacterial CpG-DNA activates dendritic cells in vivo: T helper cell-independent cytotoxic T cell responses to soluble proteins. *Eur. J. Immunol.* **30**, 3591–3597 (2000).
75. A. Lemieux, G. Sannier, A. Nicolas, M. Nayrac, G. G. Delgado, R. Cloutier, N. Brassard, M. Laporte, M. Duchesne, A. M. Sreng Flores, A. Finzi, O. Tastet, M. Dube, D. E. Kaufmann, Enhanced detection of antigen-specific T cells by a multiplexed AIM assay. *Cell Rep. Methods* **4**, 100690 (2024).
76. S. Lavazais, M. Jargosch, S. Dupont, F. Labeguere, C. Menet, C. Jagerschmidt, F. Ohm, L. Kupcsik, I. Parent, C. Cottreaux, F. Marsais, L. Oste, A. Van de Water, T. Christophe, S. De Vos, P. Fallon, F. Lauffer, P. Clement-Lacroix, K. Eyerich, R. Brys, IRAK4 inhibition dampens pathogenic processes driving inflammatory skin diseases. *Sci. Transl. Med.* **15**, eabj3289 (2023).
77. A. Bohner, M. Jargosch, N. S. Muller, N. Garzorz-Stark, C. Pilz, F. Lauffer, R. Wang, S. Roenneberg, A. Zink, J. Thomas, F. J. Theis, T. Biedermann, S. Eyerich, K. Eyerich, The neglected twin: Nummular eczema is a variant of atopic dermatitis with co-dominant  $T_H2/T_H17$  immune response. *J. Allergy Clin. Immunol.* **152**, 408–419 (2023).
78. M. I. Love, W. Huber, S. Anders, Moderated estimation of fold change and dispersion for RNA-seq data with DESeq2. *Genome Biol.* **15**, 550 (2014).

79. P. Bankhead, M. B. Loughrey, J. A. Fernandez, Y. Dombrowski, D. G. McArt, P. D. Dunne, S. McQuaid, R. T. Gray, L. J. Murray, H. G. Coleman, J. A. James, M. Salto-Tellez, P. W. Hamilton, QuPath: Open source software for digital pathology image analysis. *Sci. Rep.* **7**, 16878 (2017).